

Resonant Enhancement of Second-Harmonic Generation in the Mid-Infrared Using Localized Surface Phonon Polaritons in Subdiffractive Nanostructures

Ilya Razdolski,^{*,†} Yiguo Chen,^{‡,§} Alexander J. Giles,^{||} Sandy Gewinner,[†] Wieland Schöllkopf,[†] Minghui Hong,[§] Martin Wolf,[†] Vincenzo Giannini,[‡] Joshua D. Caldwell,^{||} Stefan A. Maier,[‡] and Alexander Paarmann^{*,†}

[†]Physikalische Chemie, Fritz-Haber-Institut der MPG, Faradayweg 4-6, 14195 Berlin, Germany

[‡]The Blackett Laboratory, Imperial College London, London SW7 2AZ, United Kingdom

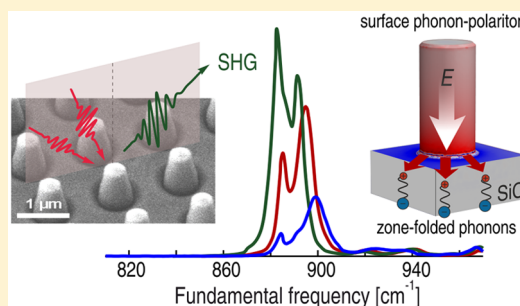
[§]Department of Electrical and Computer Engineering, National University of Singapore, 117583 Singapore

^{||}U.S. Naval Research Laboratory, 4555 Overlook Avenue SW, Washington, D.C. 20375, United States

Supporting Information

ABSTRACT: We report on the strong enhancement of mid-infrared second-harmonic generation (SHG) from SiC nanopillars due to the resonant excitation of localized surface phonon polaritons within the Reststrahlen band. A strong dependence of the SHG enhancement upon the optical mode distribution was observed. One such mode, the monopole, exhibits an enhancement that is beyond what is anticipated from field localization and dispersion of the linear and nonlinear SiC optical properties. Comparing the results for the identical nanostructures made of 4H and 6H SiC polytypes, we demonstrate the interplay of localized surface phonon polaritons with zone-folded weak phonon modes of the anisotropic crystal. Tuning the monopole mode in and out of the region where the zone-folded phonon is excited in 6H-SiC, we observe a further prominent increase of the already enhanced SHG output when the two modes are coupled. Envisioning this interplay as one of the showcase features of mid-infrared nonlinear nanophononics, we discuss its prospects for the effective engineering of nonlinear-optical materials with desired properties in the infrared spectral range.

KEYWORDS: Nonlinear optics, nanophononics, surface phonon polaritons, polar dielectrics, second harmonic generation



Light localization in subwavelength volumes is a core of nanophotonics. Conventional methods for achieving strong confinement of the electromagnetic fields extensively utilize unique properties of surface polaritons. A remarkable variety of objects and materials supporting these excitations ensures the key role of plasmonics in a broad range of applications.^{1–5} Apart from unparalleled sensitivity of plasmonic structures to the optical properties of the environment, strong light localization facilitates nonlinear-optical effects.^{6–8} Owing to the spectral tunability of the localized plasmon resonances and their sizable nonlinearity, metallic nanostructures of different shapes and sizes have earned their place in nonlinear photonics.

Despite the obvious advantages of plasmon-based nanophotonics, metallic nanoobjects exhibit significant optical losses, which lower the quality factor of the localized surface plasmon modes. Fast plasmon damping (typically on the order of 10 fs) due to ohmic losses^{9,10} thus inhibits nonlinear-optical conversion. An alternative, promising metal-free approach has been suggested, utilizing polar dielectrics such as SiC^{11–15} or BN^{16–21} for high-quality light confinement in the mid-infrared

(IR). There, the subdiffractive confinement of electromagnetic radiation relies upon surface phonon polaritons (SPhP) in the Reststrahlen band. In these material systems, electric polarization is created due to coherent oscillations of the ions instead of the electron or hole densities, as is the case in surface plasmons. Due to the significantly longer scattering times associated with optical phonons as compared to those of surface plasmons, the lifetimes of SPhPs tend to be on the order of picoseconds, orders of magnitude longer than their plasmonic counterparts.^{21,22} In addition, due to energies associated with optical phonons, SPhPs with typical frequencies within the mid-IR (>6 μm) to the THz domain hold high promise for spectroscopic and nanophotonic applications.^{23–25}

In this Letter, we undertake a first step toward the largely unexplored domain of mid-IR nonlinear nanophononics. We study the nonlinear-optical response of localized SPhPs using nanostructures made of different polytypes of SiC. Employing

Received: July 20, 2016

Revised: September 26, 2016

Published: October 21, 2016

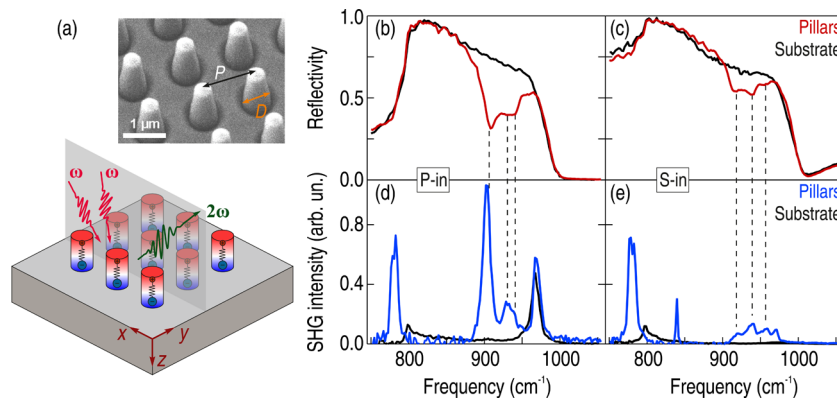


Figure 1. (a) Schematic of the experimental approach. The inset shows an electron microscopy image of the nanopillar array. (b,c) Linear reflectivity spectra for *p*- and *s*-polarized incident radiation obtained on the array of 4H-SiC nanopillars (red) and on the 4H-SiC substrate (black). (d,e) SHG excitation spectra from the 4H-SiC nanopillars (blue) and the 4H-SiC substrate (black). The vertical dashed lines indicate the excited eigenmodes of the pillars.

free electron laser (FEL) radiation in the mid-IR spectral range,²⁶ we probe second-harmonic generation from periodic arrays of subdiffractional, cylindrical SiC nanopillars. The SHG yield in the Reststrahlen band of SiC demonstrates prominent enhancement at the wavelengths associated with the excitation of the SPhP eigenmodes of the pillars. Depending on both the size and the spatial periodicity of the pillars, the SHG-probed eigenmode exhibits a spectral shift accompanied by strong variations of the SHG intensity. Analyzing different SiC polytypes, we demonstrate the interplay of the localized SPhPs with the zone-folded optical phonon modes. We further conclude that strong coupling of the two modes allows for a significant additional modulation of the SPhP-enhanced SHG output.

The schematic of our experimental approach is outlined in Figure 1a. We employed tunable FEL radiation (3 ps pulse duration, 1 μ J micropulse energy, spot size \sim 200 μ m) split into two beams to perform two-pulse correlated SHG excitation spectroscopy measurements.^{26,27} The noncollinear SHG configuration with the two beams incident at 28 and 62 degrees was used to suppress the undesirable intrinsic SHG signal generated inside the FEL cavity. Along with the SHG output, the intensity of the reflected beam incident at 62 degrees was recorded. The samples studied were square arrays of 1 μ m tall 4H-SiC and 6H-SiC pillars with the main axis of the arrays in the *xz* plane of incidence. Both 4H- and 6H-SiC samples were *c*-cut so that the *c*-axis of the crystals was parallel to the surface normal.

Typical SHG and linear reflectivity spectra collected using the FEL radiation for the two incident polarizations are presented in Figure 1b–e. There, the respective spectra of the bare substrate are shown for comparison. For *p*-polarized fundamental radiation (Figure 1d), the SHG response features two pronounced peaks located at the zone-center frequencies of transverse and longitudinal optical phonons in SiC,^{27,28} around 797 and 965 cm^{-1} , respectively. The corresponding SHG spectrum from the nanopillars demonstrate a much stronger SHG signal at around 900 cm^{-1} . Due to the absence of this peak in the SHG spectrum when the fundamental radiation is *s*-polarized, we attribute this SHG feature to the excitation of the monopole SPhP mode in the nanopillars, as this mode has previously been demonstrated to require an out-of-plane incident polarization and disappears at near-normal excitation.¹⁵ Furthermore, the multiple peaks in the SHG spectrum at

920–960 cm^{-1} are related to the excitation of the dipolar SPhP modes. Contrary to the monopole mode, these modes are observed under both *p*- and *s*-polarizations of the fundamental radiation and do not feature a strong enhancement of the normal to surface projection of the electric field E_z . This assignment of the modes is corroborated by the calculated electromagnetic field distributions, which are presented and discussed elsewhere.^{14,15}

In general, the outgoing SHG field $\vec{E}^{2\omega}$ is related to the incident electromagnetic fields E_i^ω via the so-called local field factors L_i^ω :

$$E_i^{2\omega} \propto \mathcal{P}_i^{2\omega} = \chi_{ijk}^{(2)} : (L_j^\omega E_j^\omega)(L_k^\omega E_k^\omega) \quad (1)$$

where $\mathcal{P}_i^{2\omega}$ is the nonlinear polarization and $\chi_{ijk}^{(2)}$ is the nonlinear susceptibility tensor. The excitation of the SPhP monopole mode leads to strong localization of the *z*-projection of the fundamental electric field E_z (normal to the surface plane)¹⁵ and, thus, a resonant enhancement of L_z^ω . The latter results in a pronounced increase of the SHG output when the fundamental radiation is *p*-polarized. However, the SPhP dipole modes observed in the range of 920–960 cm^{-1} rely on the resonant enhancement of the in-plane electric fields described by the local field factors $L_{x,y}^\omega$ and thus can be excited with both *p*- and *s*-polarized fundamental radiation. The total SHG response is given by a vector sum of the terms on the right-hand side of eq 1 originating from various tensor components of the nonlinear susceptibility $\chi^{(2)}$. Because the strength of $\chi_{zzz}^{(2)}$ is the largest in this spectral range,²⁸ the SPhP monopole mode, with an enhancement of L_z^ω , naturally results in a higher SHG output than the dipole modes.

The results of the systematic studies of the SHG response of various arrays of nanopillars are summarized in Figure 2 for the 4H-SiC (a,c) and 6H-SiC (b,d) samples. The a and b panels illustrate the evolution of the SHG spectra upon varying pillar diameter *D*. It is seen that upon decreasing *D*, the SPhP monopole-driven SHG peak exhibits a clear red-shift. Remarkably, although the SPhP monopole mode shifts in the range of about 890–910 cm^{-1} , the SHG enhancement factor associated with the excitation of the SPhP monopole mode varies strongly with *D*. The c and d panels offer a zoomed-in view of the evolution of the SPhP monopole mode-driven SHG for a large variety of nanopillar arrays, indicating that the variations of the SHG enhancement are observed for both 4H

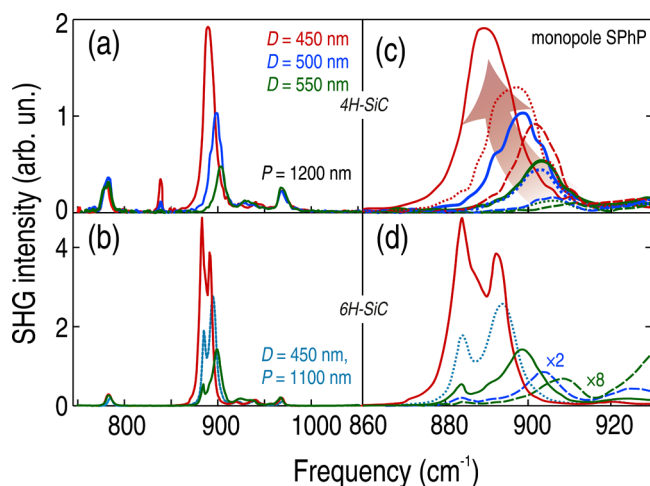


Figure 2. (a,b) Experimental p in SHG spectra for three different values of the pillar diameter D for the 4H-SiC (a) and 6H-SiC (b) samples. (c,d) Zoomed-in detail of the SHG spectra in the vicinity of the SPhP monopole resonance. Here, the colors are the same as in (a,b), and solid, dotted, and dashed lines represent $P = 1200$, 1100, and 1000 nm, respectively.

and 6H samples. The dependences of the SPhP monopole-driven SHG output on the spectral position of the SPhP monopole mode for the two SiC polytypes are shown in Figure 3a with open red squares (4H) and blue circles (6H).

Clear differences between the data obtained for the 4H- and 6H-SiC samples seen in (Figure 2c,d and Figure 3a) indicate an important role of the crystalline anisotropy for the SPhP-enhanced SHG output. The hexagonal SiC polytypes are known to exhibit zone-folded weak phonon modes in the Reststrahlen region²⁹ originating from the particular stacking of the atomic layers along the c -axis of the crystal.^{30,31} These weakly IR-active zone-folded modes can be visualized in the reflectivity measurements at oblique incidence.³² Additional periodicity of the crystals results in folding of the large Brillouin zone, thus modifying the phonon dispersion and making the excitation of phonons with nonzero wavevectors ($q \neq 0$) possible. Although zone-folded modes exist in both 4H and 6H

polytypes, different stacking of the SiC atomic layers is responsible for them having different frequencies, as illustrated in Figure 3c,d. It is seen in Figure 3d that the zone-folded mode in the 6H-SiC polytype with the reduced wave vector $q = 2/3 \pi/a$ can be excited in the range of 880–890 cm^{-1} , which is close to the typical monopole SPhP resonant frequency of the SiC nanopillars discussed above.³³ In particular, the interaction of the SPhP and zone-folded mode, which shifted the apparent spectral positions of the monopole SPhP eigenmode in the linear response,¹⁴ is seen as responsible for the complex structure of the resonant SHG output in our experiments (Figure 2d). The weak IR activity of the zone-folded modes is related to the large negative dielectric permittivity of SiC in the Reststrahlen band. As such, the out-of-plane component of the electromagnetic field E_z remains small, which inhibits the coupling of incident light to the zone-folded phonon mode. However, the excitation of the SPhP monopole mode in the nanopillars drives a strong increase of E_z , which facilitates the SPhP monopole interaction with the zone-folded phonon (Figure 3c).

The effect of the crystalline anisotropy in SiC is summarized in Figure 3a. The open symbols depict the SHG intensity obtained at the SPhP monopole (resonant) frequencies, and the dashed lines illustrate a clear correlation between the maximum SHG output and the spectral position of the SPhP monopole peak. When the SPhP monopole and the zone-folded mode start to spectrally overlap, an additional enhancement of the SHG output produced at the monopole resonance in 6H-SiC samples is observed. Moreover, the magnitude of the SHG output at the frequency of the zone-folded mode (884 cm^{-1} , green triangles) exhibits a much-faster increase when the two resonances are in close spectral proximity (dotted line), indicating an efficient interplay between the SPhP monopole and the zone-folded mode in the 6H-SiC samples. Due to the crystalline anisotropy, in 4H-SiC, the zone-folded mode is excited in a different spectral region (838 cm^{-1}), and the aforementioned mechanism remains inactive.

The strong dispersion in the SiC Reststrahlen band suggests that the observed increase of the resonant SHG enhancement upon red-shift of the SPhP resonance (common to both the 4H

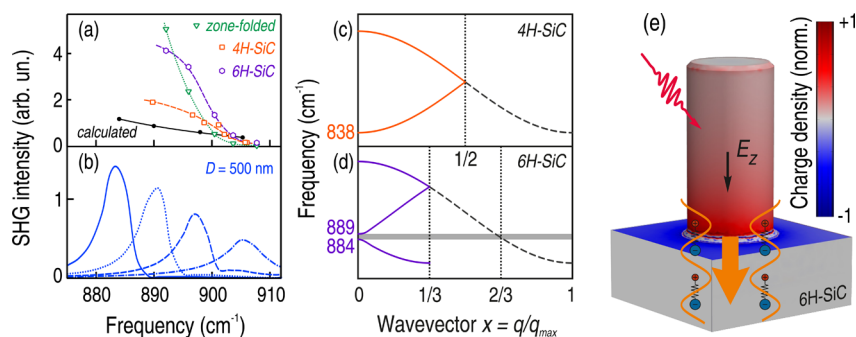


Figure 3. (a) Variations of the resonant SHG output with the fundamental frequency of the SPhP monopole mode. The data for both 4H-SiC (red squares) and 6H-SiC (blue circles) demonstrate enhancement of the SPhP monopole resonance-driven SHG when the frequency of the SPhP mode is red-shifted. The full black circles indicate the expected SHG output modulation, as obtained from the numerical simulations. (b) The green triangles demonstrate the increase of the SHG output driven by the excitation of the zone-folded mode in 6H-SiC samples. (c) Numerically simulated SHG output spectra in the vicinity of the SPhP monopole mode for the pillar diameter $D = 500$ nm and four different array periodicities, $P = 900, 1000, 1100,$ and 1200 nm. (c,d) Sketch of the dispersion of the longitudinal optical phonon modes in the full Brillouin zone and the emergence of the zone-folded modes in 4H- and 6H-SiC polytypes. Here, $q_{\text{max}} = \pi/a$, where a is the lattice period. (e) Illustration of the coupling mechanism of the zone-folded and the monopole SPhP modes via the enhanced normal to surface projection of the electric field E_z . The false color map in the background represents the calculated distribution of the electric charge when the SPhP monopole mode is excited.

and 6H systems) could be captured in numerical simulations. We calculated SHG response using both linear and nonlinear SiC dispersion,^{14,27,28} the results of the simulation of the linear optical response,¹⁵ and nonlinear polarization $\mathcal{P}^{2\omega}$ from eq 1 spatially integrated over the SiC volume (see the Supporting Information for details), with the following nonzero components of the nonlinear susceptibility: $\chi_{zzz}^{(2)}$, $\chi_{zxx}^{(2)}$, and $\chi_{xxz}^{(2)} = \chi_{xxz}^{(2)}$. The resultant SHG spectra simulated with COMSOL multiphysics software (www.comsol.com, shown in Figure 3b) demonstrate a qualitative agreement with the experimental data. However, it is seen that the steep experimental dependence cannot be quantitatively described within the simple local model used in the calculations, which yields only a moderate increase of the SHG output when the SPhP monopole mode frequency is decreased.

We note that a large mismatch between the spatial period of the nanopillars, $P \approx 1 \mu\text{m}$, and the resonant light wavelength, $\lambda \approx 10 \mu\text{m}$, rules out the excitation of propagating surface polaritons,³⁴ which are known to enhance the SHG output.^{35–39} Furthermore, Capretti et al.⁴⁰ thoroughly examined plasmon-induced SHG enhancement from arrays of Au nanoparticles as a function of the interparticle distance b . In the regime of $b < \lambda$ (as it is here), the dependence of the SHG output on b was explained in terms of the changing filling factor (and thus the associated number of active nanoemitters). For very small interparticle gaps ($b/\lambda \sim 10^{-2}$), a modulation of the SHG output has been attributed to the modification of the electromagnetic field localization in the gaps.⁴¹ Because all these effects are included in our simulations, we conclude that the origin of the observed disagreement is related to the intrinsic limitations of the employed model. As such, the apparent discrepancy between the experimentally observed trend and the results of numerical simulations suggests the need for a novel theoretical description. The latter could profit from taking into account terms in the multipole expansion of the nonlinear polarization $\mathcal{P}^{2\omega}$ beyond the bulk electric dipole one. In particular, this theory could include (i) surface SHG contributions arising from the additional symmetry breaking at the SiC–air interface and (ii) modifications of the nonlocal SHG contributions. The importance of the nonlocal SHG, already demonstrated in a number of works on subwavelength plasmonic nanoobjects,^{41–48} relies on the large gradients of the strongly localized electric field ∇E . Furthermore, intrinsic excitations capable of coupling to SPhPs, such as zone-folded modes, need to be accounted for as well to provide an accurate description of the SHG output from different SiC polytypes. The development of such calculational framework, which is beyond the scope of this publication, could provide a significant boost to the emerging field of mid-IR nonlinear nanophononics.

We note that the interaction of the localized SPhP eigenmodes and the intrinsic excitations of the medium is a unique fingerprint of mid-IR nanophononics. Indeed, surface plasmon excitations in metals rely on the free electron gas, which is essentially isotropic. As such, the SHG output of plasmonic nanostructures is (i) largely determined by the metal of choice, usually Au, (ii) exhibits only weak spectral dependence,^{40,49} and (iii) is limited by robust phase relations in the likely case of multiple SHG sources.^{47,50–53} On the contrary, the flexibility of the SPhPs is provided by the coupling of the surface phonon polariton excitations to the intrinsic bulk phonon modes. The latter can be engineered by designing

artificial metamaterials based on hybrid multilayer structures,^{54,55} thus allowing for an effective control of their optical properties.

To summarize, we have observed SHG output enhancement associated with the excitation of the SPhP eigenmodes in an array of nanopillars grown from SiC of different polytypes. The strongest SHG output is associated with the excitation of the monopole SPhP mode characterized by strong localization of the normal to surface projection of the electric field E_z . The spectral positions of the SHG peaks shift according to the geometric parameters of the nanophononic structures. We found a strong dependence of the magnitude of the SHG enhancement on the resonant frequency. This experimentally observed dependence cannot be quantitatively described by simply taking into account the subdiffractive field localization and the dispersion of the linear and nonlinear optical properties of SiC. Furthermore, we discuss the interplay of the SPhPs and the intrinsic crystalline anisotropy for an efficient nonlinear-optical conversion. This mechanism is supported by the SHG spectral measurements on the 6H-SiC nanopillars, where excitation of the SPhP monopole mode interacting with the weak zone-folded phonon resulted in an additional enhancement of the SHG output. The presence of intrinsic resonances strongly alters the phase relations in their vicinity, providing a natural way of optimizing the SHG response in a relatively narrow spectral range. Our findings demonstrate the high potential of mid-IR nonlinear nanophononics as a novel and promising platform for nonlinear optics and illustrate the rich opportunities it provides for efficient control over nonlinear-optical response.

■ ASSOCIATED CONTENT

§ Supporting Information

The Supporting Information is available free of charge on the ACS Publications website at DOI: 10.1021/acs.nanolett.6b03014.

Details of the experimental setup, estimate of the SHG conversion efficiency, details of the numerical calculations, and SiC dielectric function at the frequencies of the resonance. (PDF)

■ AUTHOR INFORMATION

Corresponding Authors

*E-mail: razdolski@fhi-berlin.mpg.de.

*E-mail: alexander.paarmann@fhi-berlin.mpg.de.

Present Address

¹NRC Postdoctoral Fellow, residing at Naval Research Laboratory, Washington, D. C. 20375, United States

Notes

The authors declare no competing financial interest.

■ ACKNOWLEDGMENTS

The authors thank G. Kichin and A. Kirilyuk (Radboud University Nijmegen) for stimulating discussions. S.A.M. acknowledges the Office of Naval Research, the Royal Society, and the Lee–Lucas Chair in Physics. A.J.G. acknowledges financial support from the NRC–NRL Postdoctoral Fellowship Program. Funding for J.D.C. was provided by the Office of Naval Research through the Naval Research Laboratory's Nanoscience Institute.

■ REFERENCES

- (1) Barnes, W. L.; Dereux, A.; Ebbesen, T. W. Surface plasmon subwavelength optics. *Nature (London, U. K.)* **2003**, *424*, 824–830.
- (2) Maier, S. A. *Plasmonics: Fundamentals and Applications*; Springer: New York, 2007.
- (3) Schuller, J. A.; Barnard, E. S.; Cai, W.; Jun, Y. C.; White, J. S.; Brongersma, M. L. Plasmonics for extreme light concentration and manipulation. *Nat. Mater.* **2010**, *9*, 193–204.
- (4) Boriskina, S. V.; Ghasemi, H.; Chen, G. Plasmonic materials for energy: From physics to applications. *Mater. Today* **2013**, *16*, 375–386.
- (5) Brongersma, M. L.; Halas, N. J.; Nordlander, P. Plasmon-induced hot carrier science and technology. *Nat. Nanotechnol.* **2015**, *10*, 25–34.
- (6) Kauranen, M.; Zayats, A. V. Nonlinear Plasmonics. *Nat. Photonics* **2012**, *6*, 737–748.
- (7) Hentschel, M.; Utikal, T.; Metzger, B.; Giessen, H.; Lippitz, M. In *Progress in Nonlinear Nano-Optics*; Sabake, S., Lienau, C., Grunwald, R., Eds.; Springer International Publishing: Switzerland, 2015; Chapter 9, pp 153–181.
- (8) Butet, J.; Brevet, P.-F.; Martin, O. J. F. Optical Second Harmonic Generation in Plasmonic Nanostructures: From Fundamental Principles to Advanced Applications. *ACS Nano* **2015**, *9*, 10545–10562.
- (9) Vahala, K. J. Optical microcavities. *Nature (London, U. K.)* **2003**, *424*, 839–846.
- (10) Barnes, W. L. Surface plasmon-polariton length scales: a route to sub-wavelength optics. *J. Opt. A: Pure Appl. Opt.* **2006**, *8*, S87–S93.
- (11) Greffet, J.-J.; Carminati, R.; Joulain, K.; Mulet, J.-P.; Mainguy, S.; Chen, Y. Coherent emission of light by thermal sources. *Nature (London, U. K.)* **2002**, *416*, 61–64.
- (12) Hillenbrand, R.; Taubner, T.; Keilmann, F. Phonon-enhanced light-matter interaction at the nanometre scale. *Nature (London, U. K.)* **2002**, *418*, 159–162.
- (13) Neuner, B., III; Korobkin, D.; Fietz, C.; Carole, D.; Ferro, G.; Shvets, G. Critically coupled surface phonon-polariton excitation in silicon carbide. *Opt. Lett.* **2007**, *34*, 2667–2669.
- (14) Caldwell, J. D.; Glembocki, O. J.; Francescato, Y.; Sharac, N.; Giannini, V.; Bezares, F. J.; Long, J. P.; Owrutsky, J. C.; Vurgaftman, I.; Tischler, J. G.; Wheeler, V. D.; Bassim, N. D.; Shirey, L. M.; Kasica, R.; Maier, S. A. Low-Loss, Extreme Subdiffraction Photon Confinement via Silicon Carbide Localized Surface Phonon Polariton Resonators. *Nano Lett.* **2013**, *13*, 3690–3697.
- (15) Chen, Y.; Francescato, Y.; Caldwell, J. D.; Giannini, V.; Maß, T. W. W.; Glembocki, O. J.; Bezares, F. J.; Taubner, T.; Kasica, R.; Hong, M.; Maier, S. A. Spectral tuning of localized surface phonon polariton resonators for low-loss mid-IR applications. *ACS Photonics* **2014**, *1*, 718–724.
- (16) Caldwell, J. D.; Kretinin, A. V.; Chen, Y.; Giannini, V.; Fogler, M. M.; Francescato, Y.; Ellis, C. T.; Tischler, J. G.; Woods, C. R.; Giles, A. J.; Hong, M.; Watanabe, K.; Taniguchi, T.; Maier, S. A.; Novoselov, K. S. Sub-diffractive volume-confined polaritons in the natural hyperbolic material hexagonal boron nitride. *Nat. Commun.* **2014**, *5*, 5221.
- (17) Dai, S.; et al. Tunable phonon polaritons in atomically thin van der Waals crystals of boron nitride. *Science* **2014**, *343*, 1125–1129.
- (18) Caldwell, J. D.; Vurgaftman, I.; Tischler, J. G. Probing hyperbolic polaritons. *Nat. Photonics* **2015**, *9*, 638–640.
- (19) Li, P.; Lewin, M.; Kretinin, A. V.; Caldwell, J. D.; Novoselov, K. S.; Taniguchi, T.; Watanabe, K.; Gaussmann, F.; Taubner, T. Hyperbolic phonon-polaritons in boron nitride for near-field optical imaging and focusing. *Nat. Commun.* **2015**, *6*, 7507.
- (20) Dai, S.; Ma, Q.; Andersen, T.; McLeod, A. S.; Fei, Z.; Liu, M. K.; Wagner, M.; Watanabe, K.; Taniguchi, T.; Thieme, M.; Keilmann, F.; Jarillo-Herrero, P.; Fogler, M. M.; Basov, D. N. Subdiffractional focusing and guiding of polaritonic rays in a natural hyperbolic material. *Nat. Commun.* **2015**, *6*, 6963.
- (21) Yoxall, E.; Schnell, M.; Nikitin, A. Y.; Txoperena, O.; Woessner, A.; Lundberg, M. B.; Casanova, F.; Hueso, L. E.; Koppens, F. H. L.; Hillenbrand, R. Direct observation of ultraslow hyperbolic polariton propagation with negative phase velocity. *Nat. Photonics* **2015**, *9*, 674–678.
- (22) Caldwell, J. D.; Lindsay, L.; Giannini, V.; Vurgaftman, I.; Reinecke, T. L.; Maier, S. A.; Glembocki, O. J. Low-loss, infrared and terahertz nanophotonics using surface phonon polaritons. *Nanophotonics* **2015**, *4*, 44–68.
- (23) Ferguson, B.; Zhang, X.-C. Materials for terahertz science and technology. *Nat. Mater.* **2002**, *1*, 26–33.
- (24) Ulbricht, R.; Hendry, E.; Shan, J.; Heinz, T. F.; Bonn, M. Carrier dynamics in semiconductors studied with time-resolved terahertz spectroscopy. *Rev. Mod. Phys.* **2011**, *83*, 543–586.
- (25) Kampfrath, T.; Tanaka, K.; Nelson, K. A. Resonant and nonresonant control over matter and light by intense terahertz transients. *Nat. Photonics* **2013**, *7*, 680–690.
- (26) Schöllkopf, W.; Gewinner, S.; Junkes, H.; Paarmann, A.; von Helden, G.; Bluem, H.; Todd, A. M. The new IR and THz FEL facility at the Fritz Haber Institute in Berlin. *Proc. SPIE* **2015**, *9512*, 95121L.
- (27) Paarmann, A.; Rzdolski, I.; Melnikov, A.; Gewinner, S.; Schöllkopf, W.; Wolf, M. Second harmonic generation spectroscopy in the Reststrahl band of SiC using an infrared free-electron laser. *Appl. Phys. Lett.* **2015**, *107*, 081101.
- (28) Paarmann, A.; Rzdolski, I.; Gewinner, S.; Schoellkopf, W.; Wolf, M. Effects of Crystal Anisotropy on Optical Phonon Resonances in the Mid-Infrared Second Harmonic Response of SiC. *Phys. Rev. B*, accepted for publication. DOI: [10.1103/PhysRevB.00.004300](https://doi.org/10.1103/PhysRevB.00.004300).
- (29) Bluet, J.; Chourou, K.; Anikin, M.; Madar, R. Weak phonon modes observation using infrared reflectivity for 4H, 6H and 15R polytypes. *Mater. Sci. Eng., B* **1999**, *B61–62*, 212–216.
- (30) Patrick, L. Infrared Absorption in SiC Polytypes. *Phys. Rev.* **1968**, *167*, 809–813.
- (31) Feldman, D. W.; Parker, J. H., Jr.; Choyke, W. J.; Patrick, L. Phonon Dispersion Curves by Raman Scattering in SiC, Polytypes 3C, 4H, 6H, 15R, and 21R. *Phys. Rev.* **1968**, *173*, 787–793.
- (32) Engelbrecht, F.; Helbig, R. Effect of crystal anisotropy on the infrared reflectivity of 6H-SiC. *Phys. Rev. B: Condens. Matter Mater. Phys.* **1993**, *48*, 15698–15707.
- (33) Despite the zone-folded mode in 6H-SiC is split into two, we only observe distinct SHG output from the one at 884 cm⁻¹.
- (34) Raether, H. *Surface Plasmons on Smooth and Rough Surfaces and on Gratings*; Springer-Verlag: Berlin, Germany, 1988.
- (35) Agarwal, G. S.; Jha, S. S. Surface-enhanced second-harmonic generation at a metallic grating. *Phys. Rev. B: Condens. Matter Mater. Phys.* **1982**, *26*, 482.
- (36) Coutaz, J. Experimental study of second-harmonic generation from silver gratings of various groove depths. *J. Opt. Soc. Am. B* **1987**, *4*, 105–106.
- (37) Quail, J. C.; Simon, H. J. Second-harmonic generation from a silver grating with surface plasmons. *J. Opt. Soc. Am. B* **1988**, *5*, 325–329.
- (38) Rzdolski, I.; Parchenko, S.; Stupakiewicz, A.; Semin, S.; Stognij, A.; Maziewski, A.; Kirilyuk, A.; Rasing, T. Second-Harmonic Generation from a Magnetic Buried Interface Enhanced by an Interplay of Surface Plasma Resonances. *ACS Photonics* **2015**, *2*, 20–26.
- (39) Gubbin, C. R.; Martini, F.; Politi, A.; Maier, S. A.; De Liberato, S. Strong and Coherent Coupling between Localized and Propagating Phonon Polaritons. *Phys. Rev. Lett.* **2016**, *116*, 246402.
- (40) Capretti, A.; Walsh, G. F.; Minissale, S.; Trevino, J.; Forestiere, C.; Miano, G.; Dal Negro, L. Multipolar second harmonic generation from planar arrays of Au nanoparticles. *Opt. Express* **2012**, *20*, 15797–15806.
- (41) Canfield, B. K.; Husu, H.; Laukkanen, J.; Bai, B.; Kuittinen, M.; Turunen, J.; Kauranen, M. Local Field Asymmetry Drives Second-Harmonic Generation in Noncentrosymmetric Nanodimers. *Nano Lett.* **2007**, *7*, 1251–1255.
- (42) Shan, J.; Dadap, J.; Stiopkin, I.; Reider, G.; Heinz, T. Experimental study of optical second-harmonic scattering from

spherical nanoparticles. *Phys. Rev. A: At., Mol., Opt. Phys.* **2006**, *73*, 023819.

(43) Kujala, S.; Canfield, B. K.; Kauranen, M.; Svirko, Y.; Turunen, J. Phonon-enhanced light-matter interaction at the nanometre scale. *Phys. Rev. Lett.* **2007**, *98*, 167403.

(44) Bachelier, G.; Butet, J.; Russier-Antoine, I.; Jonin, C.; Benichou, E.; Brevet, P.-F. Origin of optical second-harmonic generation in spherical gold nanoparticles: Local surface and nonlocal bulk contributions. *Phys. Rev. B: Condens. Matter Mater. Phys.* **2010**, *82*, 235403.

(45) Butet, J.; Bachelier, G.; Russier-Antoine, I.; Jonin, C.; Benichou, E.; Brevet, P.-F. Interference between Selected Dipoles and Octupoles in the Optical Second-Harmonic Generation from Spherical Gold Nanoparticles. *Phys. Rev. Lett.* **2010**, *105*, 077401.

(46) Rzdolski, I.; Gheorghe, D. G.; Melander, E.; Hjörvarsson, B.; Patoka, P.; Kimel, A. V.; Kirilyuk, A.; Papaioannou, E. T.; Rasing, T. Nonlocal nonlinear magneto-optical response of a magnetoplasmonic crystal. *Phys. Rev. B: Condens. Matter Mater. Phys.* **2013**, *88*, 075436.

(47) Kruk, S.; Weismann, M.; Bykov, A. Y.; Mamonov, E. A.; Kolmychek, I. A.; Murzina, T.; Panoiu, N. C.; Neshev, D. N.; Kivshar, Y. S. Enhanced Magnetic Second-Harmonic Generation from Resonant Metasurfaces. *ACS Photonics* **2015**, *2*, 1007–1012.

(48) Hille, A.; Moeferd, M.; Wolff, C.; Matyssek, C.; Rodriguez-Oliveros, R.; Prohm, C.; Niegemann, J.; Grafstrom, S.; Eng, L. M.; Busch, K. Second Harmonic Generation from Metal Nano-Particle Resonators: Numerical Analysis On the Basis of the Hydrodynamic Drude Model. *J. Phys. Chem. C* **2016**, *120*, 1163–1169.

(49) Metzger, B.; Gui, L.; Fuchs, J.; Floess, D.; Hentschel, M.; Giessen, H. Strong Enhancement of Second Harmonic Emission by Plasmonic Resonances at the Second Harmonic Wavelength. *Nano Lett.* **2015**, *15*, 3917–3922.

(50) Husu, H.; Canfield, B. K.; Laukkanen, J.; Bai, B.; Kuittinen, M.; Turunen, J.; Kauranen, M. Local-field effects in the nonlinear optical response of metamaterials. *Metamaterials* **2008**, *2*, 155–168.

(51) Palomba, S.; Novotny, L. Nonlinear excitation of surface plasmon polaritons by four-wave mixing. *Phys. Rev. Lett.* **2008**, *101*, 056802.

(52) Capretti, A.; Forestiere, C.; Dal Negro, L.; Miano, G. Full-Wave Analytical Solution of Second-Harmonic Generation in Metal Nanospheres. *Plasmonics* **2014**, *9*, 151–166.

(53) Rzdolski, I.; Makarov, D.; Schmidt, O. G.; Kirilyuk, A.; Rasing, T.; Temnov, V. V. Nonlinear Surface Magnetoplasmonics in Kretschmann Multilayers. *ACS Photonics* **2016**, *3*, 179–183.

(54) Dai, S.; et al. Graphene on hexagonal boron nitride as a tunable hyperbolic metamaterial. *Nat. Nanotechnol.* **2015**, *10*, 682–687.

(55) Caldwell, J. D.; Vurgaftman, I.; Tischler, J. G.; Glembocki, O. J.; Owrutsky, J. C.; Reinecke, T. L. Atomic-scale photonic hybrids for mid-infrared and terahertz nanophotonics. *Nat. Nanotechnol.* **2016**, *11*, 9–15.